

An extended AVHRR 8-km NDVI dataset compatible with MODIS and SPOT vegetation NDVI data

COMPTON J. TUCKER, JORGE E. PINZON, MOLLY E. BROWN*, DANIEL
A. SLAYBACK, EDWIN W. PAK, ROBERT MAHONEY, ERIC F. VERMOTE
and NAZMI EL SALEOUS

Laboratory for Terrestrial Physics, Biospheric Sciences Branch, Code 923, NASA/
Goddard Space Flight Center, Greenbelt, Maryland 20771 USA

(Received 28 July 2004; in final form 18 March 2005)

Daily daytime Advanced Very High Resolution Radiometer (AVHRR) 4-km global area coverage data have been processed to produce a Normalized Difference Vegetation Index (NDVI) 8-km equal-area dataset from July 1981 through December 2004 for all continents except Antarctica. New features of this dataset include bimonthly composites, NOAA-9 descending node data from August 1994 to January 1995, volcanic stratospheric aerosol correction for 1982–1984 and 1991–1993, NDVI normalization using empirical mode decomposition/reconstruction to minimize varying solar zenith angle effects introduced by orbital drift, inclusion of data from NOAA-16 for 2000–2003 and NOAA-17 for 2003–2004, and a similar dynamic range with the MODIS NDVI. Two NDVI compositing intervals have been produced: a bimonthly global dataset and a 10-day Africa-only dataset. Post-processing review corrected the majority of dropped scan lines, navigation errors, data drop outs, edge-of-orbit composite discontinuities, and other artefacts in the composite NDVI data. All data are available from the University of Maryland Global Land Cover Facility (<http://glcf.umiaccs.umd.edu/data/gimms/>).

1. Introduction

New improved coarse-resolution global land surface satellite sensor data are available from SPOT-4's Vegetation instrument (May 1998 to present) and NASA's Moderate Resolution Imaging Spectrometers (MODIS) on the Terra and Aqua platforms (January 2000 to present and December 2002 to present, respectively) (table 1). Although significant improvements have been made with new global land vegetation-sensing instruments, the existing July 1981 to the present 4-km archive of data from the Advanced Very High Resolution Radiometer (AVHRR) instrument is an invaluable and irreplaceable archive of historical land surface information. This archive of global 4-km AVHRR data results from six different AVHRR instruments on six different NOAA polar-orbiting meteorological satellites (Cracknell 1997, Kidwell 1997). If the 1981–2004 record of AVHRR data could be processed in a consistent and quantitatively comparable manner with the new generation of sensors mentioned above, the global land surface satellite climate data record

*Corresponding author. Email: molly.brown@gsfc.nasa.gov

Table 1. Global coarse-resolution satellite spectral vegetation index datasets. Data from these satellites can be used to study the photosynthetic capacity of vegetation from space. The Sea-viewing Wide Field-of-view Sensor (SeaWiFS) data are also included because these data are also available globally for the SeaWiFS era.

Instrument	Dates of coverage	Spatial resolution (nadir)	No. of spectral bands	Global data volume (gb/day)	References, comments
<i>NOAA AVHRR</i>					
NOAA-7	Jul. 1981–Feb. 1985	4 km	5	0.6	Cracknell (1997), Kidwell (1997)
NOAA-9	Feb. 1985–Sep. 1988	4 km	5	0.6	
NOAA-11	Sep. 1988–Aug. 1994	4 km	5	0.6	No data after September 1994
NOAA-9-d	Aug. 1994–Jan. 1995	4 km	5	0.6	Descending node 09:00 data
NOAA-14	Jan. 1995–Nov. 2000	4 km	5	0.6	
NOAA-16	Nov. 2000 to present	4 km	5	0.6	
SeaWiFS	Sep. 1997 to present	4 km	8	0.4	Hooker <i>et al.</i> (1992)
SPOT-4 Vegetation	May 1998 to present	1 km	4	5	Saint (1995)
MODIS	Jan. 2000 to present	250–1000 m	32	76/instrument	Justice <i>et al.</i> (1998)

acquires an additional ≈ 19 years to complement the 6+ years of data presently in hand from the improved sensors listed in table 1.

2. Spectral vegetation indices

Spectral vegetation indices are usually composed of red and near-infrared radiances or reflectances (Tucker 1979), sometimes with additional channels included, and are one of the most widely used remote sensing measurements (Cracknell 2001). They are highly correlated with the photosynthetically active biomass, chlorophyll abundance, and energy absorption (reviewed in Myneni *et al.* 1995). The use of spectral vegetation indices derived from AVHRR satellite data followed the launch of NOAA-6 in June 1979 and NOAA-7 in July 1981 (Gray and McCrary 1981, Schneider *et al.* 1981, Townshend and Tucker 1981). The AVHRR instruments on NOAA-6 and NOAA-7 were the first in the TIROS-N series of satellites to have non-overlapping channel 1 and channel 2 spectral bands. Overlapping red and near-infrared spectral bands precludes calculating a NDVI. The NDVI is calculated as $NDVI = (\text{channel } 2 - \text{channel } 1) / (\text{channel } 2 + \text{channel } 1)$.

The Normalized Difference Vegetation Index (NDVI) has become the most used product derived from NOAA AVHRR data (Cracknell 2001), largely from the use of NDVI datasets formed via maximum value compositing (Holben 1986). AVHRR NDVI data have been used extensively since 1981 to study a variety of global land processes (reviewed in Townshend 1994, D'Souza *et al.* 1996, Cracknell 1997, and Defries and Belward 2000, among others). This was never anticipated by the designers of the AVHRR instruments who had no idea what a vegetation index was.

Vegetation indices from SPOT Vegetation and from the MODIS instruments represent improved measurements of surface vegetation conditions, spatially, spectrally, and radiometrically. The spectral bandwidth differences are apparent in figure 1, where the first two AVHRR channels span considerable spectral intervals compared to the other instruments in this figure. This complicates *ex post facto* absolute calibration of the AVHRR reflective channels and makes atmospheric correction more difficult (Tanre *et al.* 1992) because spectral response within a channel can change over time.

Previous AVHRR-derived global land surface NDVI data include the NOAA Global Vegetation Index (GVI) (Tarpley *et al.* 1984), the NASA Pathfinder 8-km dataset (James and Kalluri 1994), and a dataset produced by the European Space Agency at the Joint Research Center in Italy (Malingreau and Belward 1994). Tucker *et al.* (1994) and Los *et al.* (1994) described early AVHRR NDVI datasets produced at NASA/Goddard Space Flight Center. AVHRR 1-km land surface datasets were produced for a limited time by Eidenshink and Faundeen (1994). We now describe a new AVHRR NDVI dataset available to the research community.

3. Data processing

Satellite sensor data in NOAA level-1b format (Kidwell 1997) were ingested, all data with scan angles $< \pm 40^\circ$ from nadir were forward mapped to the output bin closest to the centre location of each 8 km equal area grid cell, respective calibration values were applied, and the maximum NDVI retained for each compositing period.

We used a similar navigation procedure to Saleous *et al.* (2000), which in turn is based upon the work of Baldwin and Emery (1995). The orbital model predicts the

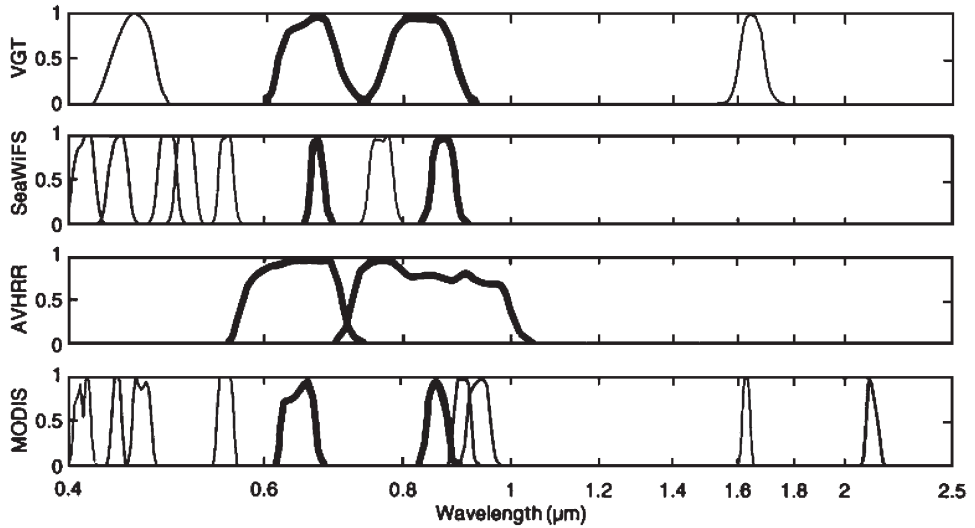


Figure 1. Spectral acceptance of the AVHRR instruments in comparison to SPOT Vegetation (VGT), SeaWiFS, and the MODIS visible and near-infrared bands. The darker spectral acceptance bands are those bands used to calculate NDVIs. Differences in spectral bandwidth and spectral acceptance functions will result in identical surface reflectances producing different NDVIs. See also table 1.

position of the satellite at any time, using the satellite on-board clock and orbital elements to determine the predicted position. From this perspective, the sun–target–sensor geometry is determined. The NOAA satellites' velocity with respect to the Earth's surface is $\approx 7 \text{ km s}^{-1}$ and the output bin size employed was 8 km. This translates into a timing error of $< \pm 1.0 \text{ s}$ to achieve a navigation accuracy of $< \pm 1$ pixel. The majority of the navigation errors were due to errors of the spacecraft clock.

Maximum value NDVI composites (Holben 1986) were formed globally by continent with a bimonthly time step and for Africa only with a 10-day time step. Data were formed into the bimonthly composite images, from the first day of the month through the 15th day and from day 16 to the end of each month for all continents. The Africa subset of the data was also formed into NDVI composite images, from the first day of the month to the 10th day, from the 11th day to the 20th, and from the 21st day to the end of the month, respectively.

Every composite image was manually checked for navigation accuracy by comparing the mapped data to a reference coastline for every continent. Images with $> \pm 1$ pixel navigation error were investigated and the day(s) of the navigation error identified. These days were reprocessed separately, manually registered to the reference data, and a new composite image reconstructed by maximum value NDVI compositing. In some cases it was necessary to discard data from specific days, as the navigation errors were impossible to adjust. We also scrutinized every composite image for data drop outs, bad scan lines, and other strange values in the data and corrected the majority of these problems.

With the failure of NOAA-13 to achieve orbit in 1992, NOAA-11 continued to provide global afternoon/early morning AVHRR data. By 1994, the afternoon

equatorial overpass time for NOAA-11 was $\approx 17:00$ hours. We began using NOAA-9 descending node AVHRR data for our global NDVI dataset in August 1994, and continued using these data until NOAA-14 became operational in late January 1995. NOAA-9 had a daytime descending node equatorial crossing time of $\approx 09:00$ hours in mid-1994 to early 1995. It had ‘rocked around the clock’, with a ≈ 3 min month⁻¹ later time procession from its original night-time descending node equatorial crossing time of 02:30 hours.

There is a difference between the Pathfinder AVHRR Land (PAL) and GVI datasets and the NDVI dataset described herein: we use NOAA-9 AVHRR data from October 1994 into January 1995 when there were no NOAA-11 AVHRR data (it had failed), and use NOAA-9 AVHRR data in August and September 1994 when the PAL and GVI datasets use NOAA-11 data.

4. Radiometric calibration

Satellite determination of long-term NDVI surface trends requires precision within and among various space-borne instruments. It is also crucial to document the within- and among-sensor calibration uncertainty to determine the accuracy with which surface trends over time can be ascertained. The NDVI data we describe were processed in two ways: (1) NOAA-7 through NOAA-14 channel 1 and 2 data were processed using the Vermote and Kaufman (1995) channel 1 and channel 2 calibration and the NDVI formed. The resulting NDVI fields were further adjusted using the technique of Los (1998), then decomposed and reconstructed using empirical mode decomposition to correct for solar zenith angle effects (Pinzon *et al.* 2004); and (2) data from NOAA-16 and NOAA-17 were processed using the preflight channel 1 and channel 2 calibration values and formed into maximum value composites. An empirical mode decomposition and reconstruction was performed that ensures a zero slope with respect to time in desert areas and was also used to correct solar zenith angle artefacts. The NOAA-16 and -17 NDVI time series were next adjusted by a constant offset to match up with a coincident-in-time and spatially aggregated 8-km SPOT Vegetation NDVI time series, which had previously been adjusted to match up with the corresponding coincident-in-time NOAA-14 NDVI time series. We thus used overlapping SPOT Vegetation NDVI time series as the means to intercalibrate or tie together the NOAA-14 and NOAA-16 and -17 NDVI time series (Pinzon *et al.* 2004). This was necessary because the bi-linear gain for channel 1 and channel 2 of NOAA-16’s and -17’s AVHRR instruments complicate *ex post facto* calibration.

5. Atmospheric correction and cloud screening

We chose to produce a maximum value NDVI composite dataset without any atmospheric correction except during the El Chichon and Mt Pinatubo volcanic stratospheric aerosol periods. A stratospheric aerosol correction was applied as proposed by Vermote *et al.* (1997) from April 1982 through December 1984 and from June 1991 through December 1993. We formed composite stratospheric aerosol optical depth fields by combining the work of Sato *et al.* (1993), Hansen *et al.* (1995) and Vermote *et al.* (1997). Rosen *et al.* (1994), Russel *et al.* (1993) and Dutton *et al.* (1994) were used to compare specific optical depth measurements to our blended global fields. We produced optical depth fields that varied by month and degree of latitude (figure 2).

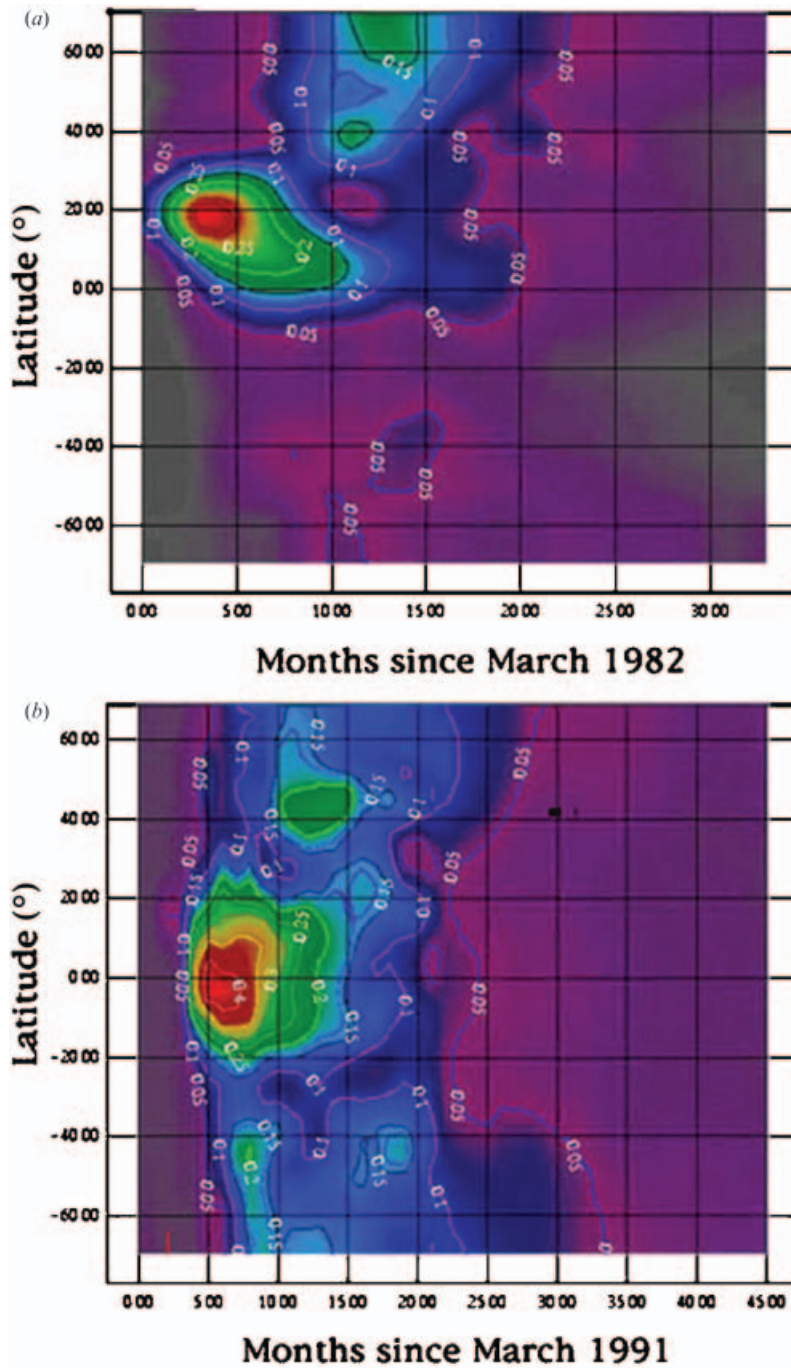


Figure 2. Stratospheric aerosol optical depth from 1982 to 1984 and 1991 to 1993. These two aerosol events were caused by the volcanic eruptions of El Chichon in 1982 and Mt Pinatubo in 1991. These data were used to correct AVHRR channel 1 and channel 2 data for the 1982–1984 and 1991–1993 periods, respectively (Vermote *et al.* 1997).

Cloud screening was provided by a channel 5 thermal mask of 0°C for all continents except Africa, where a cloud mask of 10°C was used.

Maximum value compositing was used to simultaneously minimize atmospheric and directional reflectance effects (Holben and Fraser 1984). The lack of consistently accurate atmospheric water vapour fields globally in the earlier part of the 1981–2004 AVHRR record prevented us from applying explicit atmospheric and directional reflectance corrections. We acknowledge this should be done and are working to implement these corrections in our next reprocessing of the AVHRR global data record.

6. Solar zenith angle correction

Orbital drift of the ‘afternoon’ NOAA satellites (Cracknell 1997) significantly affects sun–target–sensor geometry and introduces associated NDVI errors that vary with latitude, green leaf density, and vegetation structure (Kaufmann *et al.* 2000). We performed a solar zenith angle correction to the NDVI data using the adaptive empirical mode decomposition method of Pinzon *et al.* (2005). The empirical mode decomposition method accounts for local variation in solar zenith angle and embedded nonlinear and non-stationary variations. We are able to account for ≈90% of the solar zenith angle affect upon the NDVI at all latitudes, remove these effects from the NDVI data, and reconstruct the NDVI data without the solar zenith angle variation. Our solar zenith angle corrections were greatest in the tropics for tropical forests, moderate in the tropics for less densely vegetated areas, and lowest at higher northern and lower southern latitudes (figure 3).

7. Assessment of NDVI data quality

We assessed the quality of our new AVHRR NDVI dataset by looking at a variety of targets through time. We first compared our time series NDVI observations with desert targets at different latitudes, desert targets not used in the channel 1 and 2 calibration nor in the NDVI normalization procedure. We found the NDVI versus time trends or slopes to be very close to zero, within and among the different satellite periods, for all the deserts studied with no apparent discontinuities (figure 4).

We also compared our dataset to the Pathfinder PAL and GVI datasets. The Pathfinder AVHRR Land NDVI data (James and Kalluri 1994) and GVI data (National Climate Data Center 2003) show more interannual variation and have a different character, especially from 35° N to 35° S, than the new Global Inventory Monitoring and Modelling Study (GIMMS) NDVI data (figure 5). These differences are most pronounced from 1991 to 1994 as shown in figure 5(b). We explain these differences as the GIMMS data have a stratospheric aerosol correction for the 1991–1993 Mt Pinatubo volcanic period and use data from NOAA-9 in late 1994 rather than data from NOAA-11. In addition, the PAL and GVI data have no data from October 1994 to late January 1995, as NOAA-11’s AVHRR instrument had failed during this time. In contrast, the AVHRR NDVI data described herein used descending node ≈09:00 hours equatorial crossing time data from NOAA-9 from August 1994 until late January 1995 when NOAA-16’s AVHRR instrument came on line. It is only by comparison with well-documented ground data that the validity of any satellite retrieval of surface conditions can be established.

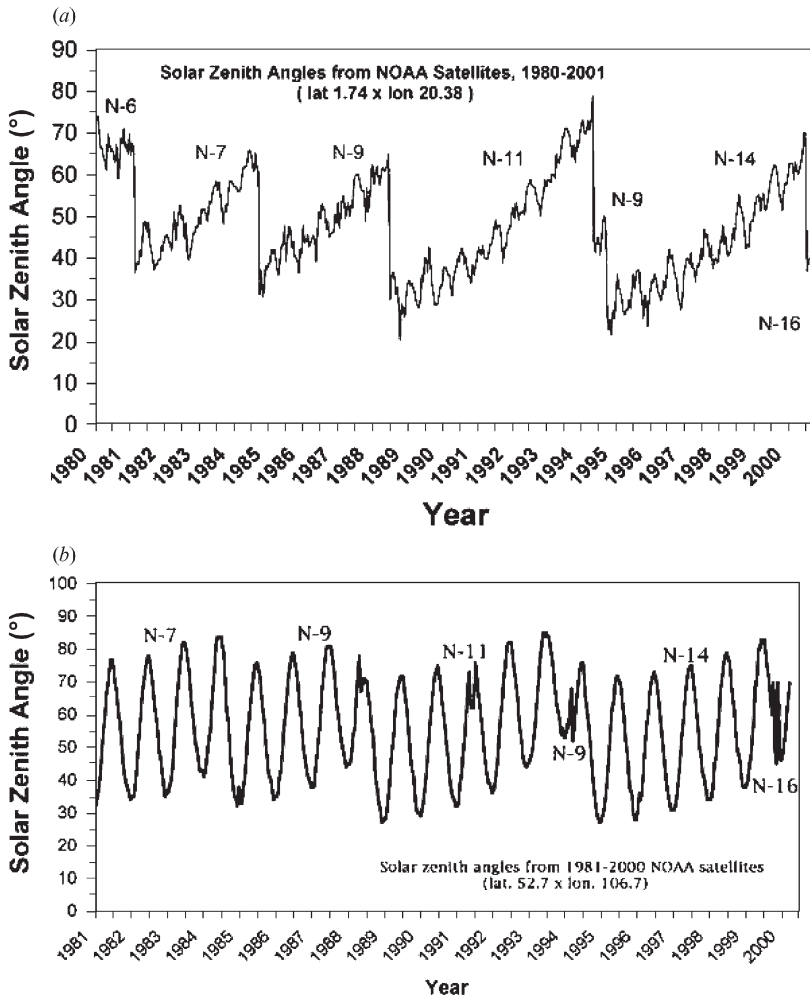


Figure 3. Solar zenith angles vs time for (a) NOAA-6 (07:30 and 19:30 hours local solar overpass times) and the series of 'afternoon' NOAA satellites from 1981 to 2003 and (b) NOAA-7 to NOAA-16 for 52.7° N. Note the procession to later overpass times in each of the afternoon satellite periods (Cracknell 1997). The very late times of NOAA-11 and NOAA-14 are comparable to the overpass time of NOAA-6 at 07:30 hours close to the equator.

The challenge when making needed corrections to the multi-instrument AVHRR NDVI continuum is to correct these data for variations in solar zenith angle, atmospheric and directional effects, stratospheric aerosols, and within and among-satellite channel 1 and 2 calibration variations without removing variation in the data caused by changing surface conditions. Previous papers by Chilar *et al.* (1998) and Gutman (1999) have questioned the non-surface uncertainty in AVHRR NDVI data.

Chilar *et al.* (1998) used 1-km AVHRR data from Canada from 1993 to 1996 and concluded the land surface Δ NDVI threshold of detection was 0.02–0.04 plus any sensor calibration errors. Considering AVHRR NDVI calibration errors over the AVHRR 1981–2004 record have been reported to be on the order of 0.02–0.04 (Vermote and Kaufman 1995), this implies the Δ NDVI threshold of detectability is

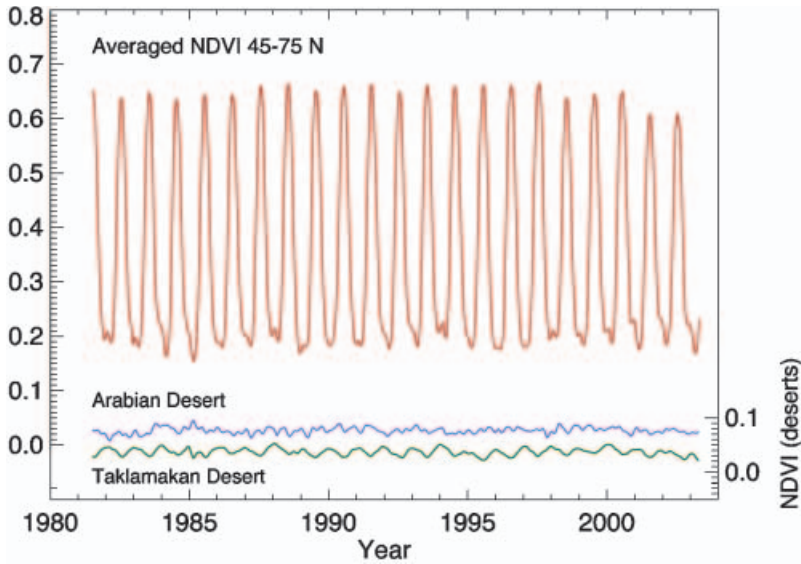


Figure 4. Time series NDVI data from the Arabian Desert (25° N, 40° E) and Taklamakan Desert (40° N, 85° E). Note that the NDVI versus time slopes for the Arabian and Taklamakan Deserts are very close to 0.00. Data from the 45° to 75° N global belt are plotted for comparison.

on the order of 0.04–0.08 NDVI units. However, Chilar *et al.* (1998) used AVHRR data with large solar zenith angles in 1994 that biased their conclusions. At 53° N latitude, the NOAA-11 data for June to August in 1994 were obtained under solar zenith angles from 53° to 63° . In contrast, the 1995 and 1996 NOAA-14 AVHRR data were obtained under solar zenith angles from 27° to 35° at 53° N latitude. Not surprisingly, most of the variation reported by Chilar *et al.* (1998) arises from their 1994 AVHRR data used, data collected under very high solar zenith angles.

We question the conclusions of Gutman (1999) who used NOAA GVI NDVI data that have introduced variability from a variety of sources including no scan angle restriction and selecting weekly composites based upon the channel 2 – channel 1 maximum difference (Goward *et al.* 1993, 1994). Gutman (1999) further: (1) assumed the Rao and Chen (1995) NOAA-9 AVHRR channel 1 and channel 2 calibrations were correct and these were used to adjust the channel 1 and channel 2 calibrations of NOAA-11 and NOAA-14; (2) assumed tropical forests have no inter-annual variation in surface reflectance; (3) ignored the Mt Pinatubo stratospheric aerosol effects in NOAA-11 data from 1991 to 1993; and (4) used NOAA-11 data from late 1994 when the equatorial overpass times were $\approx 17:00$ hours. All of these factors contribute additional variation into the GVI dataset as shown in figure 5.

The AVHRR dataset we describe differs in several important ways to previous AVHRR NDVI datasets (figure 5): we calibrated the NDVI independent of channel 1 and channel 2 absolute calibrations; we used empirical mode decomposition/reconstruction on a pixel by pixel basis independent of land cover to minimize solar zenith angle effects; we employed a stratospheric aerosol correction for 1982–1984 and 1991–1993; and we used descending node NOAA-9 AVHRR data in late 1994 and early 1995. We are presently working to reprocess the entire 1981–2005 AVHRR record to provide calibrated and corrected channels 1–5 and ancillary data to the research community.

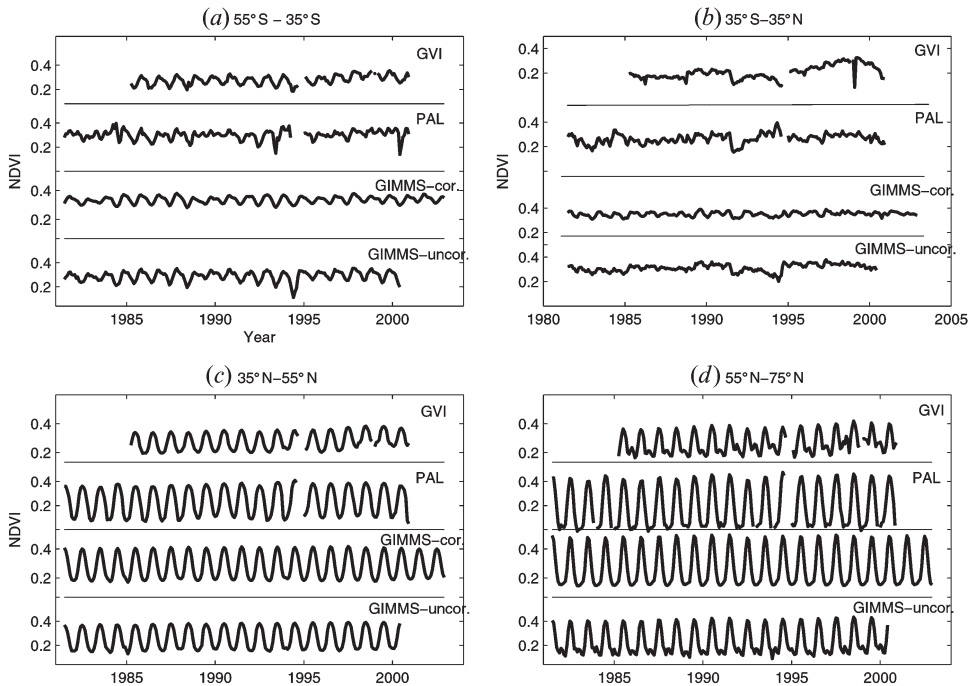


Figure 5. A comparison of different AVHRR NDVI time series by latitude zones for the 1981–2003 time period: (a) 55° S to 35° S; (b) 35° S to 35° N; (c) 35° N to 55° N; and (d) 55° N to 75° N. The PAL NDVI curves were produced from the PAL dataset distributed by the GSFC Distributed Active Archive Center (James and Kalluri 1994). The GVI curves were produced from the NOAA Global Vegetation Index (National Climate Data Center 2003). The other NDVI curves are derived from the GIMMS data we describe herein, one uncorrected for solar zenith angle effects, and the other corrected for solar zenith angle effects. Note the greater variations among these datasets closer to the equator than towards the poles. See figure 3 for solar zenith angle variations and figure 4 for NDVI desert stability of the new AVHRR global NDVI data we describe herein.

SPOT Vegetation NDVI data and MODIS NDVI data from the Terra and Aqua platforms represent improvements in the ability to monitor land photosynthetic capacity. To complement these measurements back in time, we have processed the AVHRR NDVI 1981–2004 historical record within the SPOT Vegetation NDVI and MODIS NDVI dynamic range (figure 6). This enables the many advantages of MODIS and SPOT Vegetation data to be used while retaining historical information from areas of interest, albeit at a much reduced spatial resolution.

Papers using the data we describe herein have reported stability of these data for studying 1981–2003 interannual variation of global drought phenomena (Lotsch *et al.* 2003), the effect of the 1991 Mt Pinatubo volcanic eruption upon global net primary production (Angert *et al.* 2004), the interaction of higher-latitude warming and drier summers (Angert *et al.* 2005), atmospheric circulation changes and continental drought (Buermann *et al.* 2005), interannual variability of the NDVI from Amazonia (Poveda and Salazar 2005), and the greening of arctic Alaska (Jia *et al.* 2003). All global bimonthly composite data are available from the University of Maryland's Global Land Cover Facility (<http://glcf.umiaccs.umd.edu>) and the African 10-day NDVI data are available from the Africa Data Dissemination

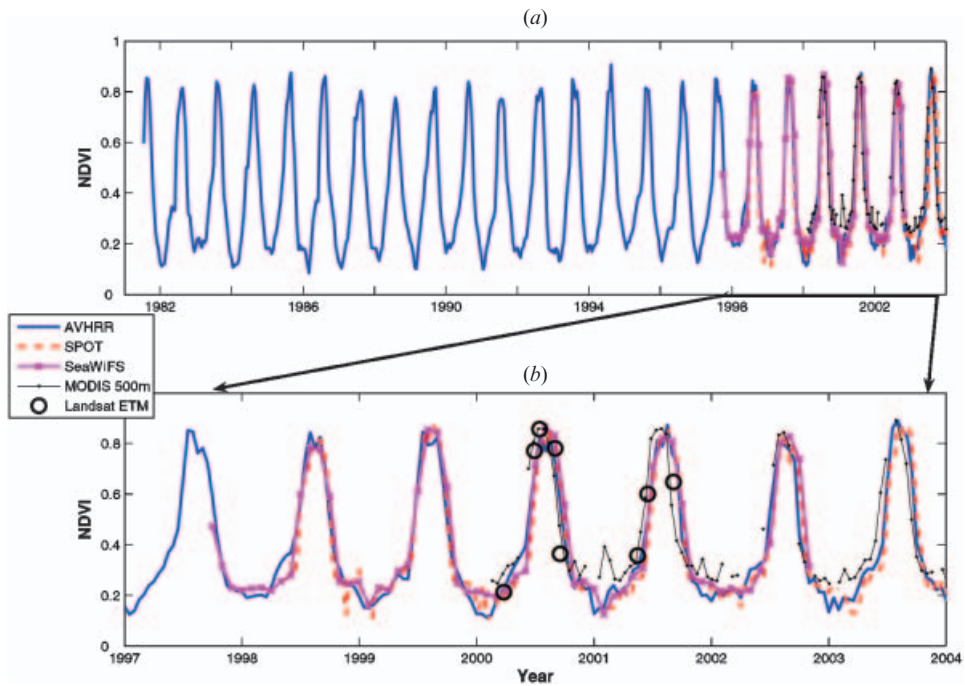


Figure 6. Bondville, Illinois time series plot with the NDVI from five sensors for (a) 1982–2004 and (b) 1997–2004. Solid blue line, the AVHRR data we describe in this paper; black line, the MODIS data; red dashed line, SPOT Vegetation data; solid red line, SeaWiFS land data; and \circ , Landsat-7 ETM data.

Service website of US AIDS' Famine Early Warning System (<http://edcsnw4.cr.usgs.gov/adds/>).

Acknowledgements

The dataset we describe would not have been possible without the work of two people: Martha Maiden and Stanley Schneider. We thank Martha Maiden of NASA Headquarters for her support that made this dataset possible. We thank Stanley Schneider for convincing NOAA management in 1977 to alter the spectral configuration of the TIROS-N channel 1 band pass from 0.55–0.90 μm to 0.55–0.70 μm . None of the extensive and widespread AVHRR NDVI work would be possible without Schneider's unilateral action in 1977 which restricted AVHRR channel 1 to the upper portion (0.55–0.70 μm) of the visible spectrum.

References

- ANGERT, A., BIRAUD, S., BONFILS, C., BUERMANN, W. and FUNG, I.Y., 2004, CO₂ seasonality indicates origins of post-Pinatubo sink. *Geophysical Research Letters*, **31**, pp. 1103–1107.
- ANGERT, A., TUCKER, C.J., BIRAUD, S., BONFILS, C., HENNING, C., BUERMANN, W. and FUNG, I.Y., 2005, Drier summers cancel out the CO₂ uptake enhancement induced by warmer winters. *Proceedings of the National Academy of Sciences USA* (in press).

- BALDWIN, D. and EMERY, W.J., 1995, Spacecraft attitude variations of NOAA-11 inferred from AVHRR imagery. *International Journal of Remote Sensing*, **16**, pp. 531–548.
- CHILAR, J., CHEN, J.M., LI, Z., HUANG, F., LATIFOVIC, R. and DIXON, R., 1998, Can interannual land surface signal be discerned in composite AVHRR data? *Journal of Geophysical Research*, **103**, pp. 23163–23172.
- CRACKNELL, A.P., 1997, *The Advanced Very High Resolution Radiometer* (London: Taylor & Francis).
- CRACKNELL, A.P., 2001, The exciting and totally unanticipated success of the AVHRR in applications for which it was never intended. *Advances in Space Research*, **28**, pp. 233–240.
- DEFRIES, R.S. and BELWARD, A.S., 2000, Global and regional land cover characterization from satellite data. *International Journal of Remote Sensing*, **21**, pp. 1083–1092.
- DUTTON, E., GREDDY, P., RYAN, S. and DELUISI, J.J., 1994, Features and effects of aerosol optical depth observed at Mauna-Loa, Hawaii—1982–1992. *Journal of Geophysical Research—Atmospheres*, **99**, pp. 8295–8306.
- D'SOUZA, G., BELWARD, A.S. and MALINGREAU, J.P., 1996, *Advances in the Use of NOAA AVHRR Data for Land Applications* (Dordrecht, The Netherlands: Kluwer).
- EIDENSHINK, J.C. and FAUDEEN, J.L., 1994, The 1 km resolution global data set: needs of the International Geosphere Biosphere Program. *International Journal of Remote Sensing*, **16**, pp. 3443–3462.
- GOWARD, S.N., DYE, D.G., TURNER, S. and YANG, J., 1993, Objective assessment of the NOAA global vegetation index data product. *International Journal of Remote Sensing*, **14**, pp. 3365–3394.
- GOWARD, S.N., TURNER, S., DYE, D.G. and LIANG, S., 1994, The University-of-Maryland Improved Global Vegetation Index product. *International Journal of Remote Sensing*, **15**, pp. 3365–3395.
- GRAY, T.I. and MCCRARY, D.G., 1981, Meteorological satellite data—a tool to describe the health of the world's agriculture. AgRISTARS Report EW-NI-04042, Johnson Space Center, Houston, Texas.
- GUTMAN, G.G., 1999, On the use of long-term global data of land reflectances and vegetation indices derived from the advanced very high resolution radiometer. *Journal of Geophysical Research*, **104**, pp. 6241–6255.
- HANSEN, J., RUEDY, J., SATO, M. and REYNOLDS, R., 1996, Global surface air temperature in 1995: return to pre-Pinatubo level. *Geophysical Research Letters*, **23**, pp. 1665–1668.
- HOLBEN, B.N., 1986, Characteristics of maximum-value composite images from temporal AVHRR data. *International Journal of Remote Sensing*, **7**, pp. 1417–1434.
- HOLBEN, B.N. and FRASER, R.S., 1984, Red and near-infrared sensor response to off-nadir viewing. *International Journal of Remote Sensing*, **5**, pp. 145–160.
- HOKER, S.B., ESAIAS, W.E., FELDMAN, G.C., GREGG, W.W. and MCCLAIN, C.R., 1992, An overview of SeaWiFS and Ocean Color. NASA Technical Memorandum 104566, vol. 1.
- JAMES, M.E. and KALLURI, S.N., 1994, The Pathfinder AVHRR land data set: an improved coarse-resolution data set for terrestrial monitoring. *International Journal of Remote Sensing*, **15**, pp. 3347–3363.
- JIA, G.J., EPSTEIN, H.E. and WALKER, D.A., 2003, Greening of arctic Alaska, 1981–2001. *Geophysical Research Letters*, **30**, pp. 1029–1033.
- JUSTICE, C.O., VERMOTE, E., TOWNSHEND, J.R.G., DEFRIES, R., ROY, D.P., HALL, D.K., SALOMONSON, V.V., PRIVETTE, J.L., RIGGS, G., STRAHLER, A., LUCHT, W., MYNENI, R.B., KNYAZIKHIN, Y., RUNNING, S.W., NEMANI, R.R., WAN, Z.M., HUETE, A.R., VAN LEEUWEN, W., WOLFE, R.E., GIGLIO, L., MULLER, J.P., LEWIS, P. and BARNESLEY, M.J., 1998, The Moderate Resolution Imaging Spectroradiometer (MODIS): land remote sensing for global change research. *IEEE Transactions on Geoscience and Remote Sensing*, **36**, pp. 1228–1249.

- KAUFMANN, R.K., ZHOU, L., KNYAZIKHIN, Y., SHABANOV, N., MYNENI, R. and TUCKER, C.J., 2000, Effect of orbital drift and sensor changes on the time series of AVHRR vegetation index data. *IEEE Transactions on Geoscience and Remote Sensing*, **38**, pp. 2584–2597.
- KIDWELL, K.B., 1997, Polar Orbiter Data Users' Guide (TIROS-n, NOAA-6, NOAA-7, NOAA-8, NOAA-9, NOAA-10, NOAA-11, NOAA-12, and NOAA-14). National Oceanic and Atmospheric Administration, Washington, DC.
- LOS, S.N., 1998, Estimation of the ratio of sensor degradation between NOAA AVHRR channels 1 and 2 from monthly NDVI composites. *IEEE Transactions on Geoscience and Remote Sensing*, **36**, pp. 206–213.
- LOS, S.O., JUSTICE, C.O. and TUCKER, C.J., 1994, A global $1^\circ \times 1^\circ$ NDVI data set for climate studies derived from the GIMMS continental NDVI data. *International Journal of Remote Sensing*, **15**, pp. 3493–3618.
- LOTSCH, A., FRIEDL, M.A., ANDERSON, B.T. and TUCKER, C.J., 2003, Coupled vegetation–precipitation variability observed from satellite and climate records. *Geophysical Research Letters*, **30**, pp. 125–132.
- MALINGREAU, J.P. and BELWARD, A.S., 1994, Recent activities in the European Community for the creation and analysis of global AVHRR data sets. *International Journal of Remote Sensing*, **15**, pp. 3397–3416.
- MYNENI, R.B., HALL, F.G., SELLERS, P.J. and MARSHAK, A.L., 1995, The interpretation of spectral vegetation indexes. *IEEE Transactions on Geoscience and Remote Sensing*, **33**, pp. 481–486.
- NATIONAL CLIMATE DATA CENTER, 2003, NOAA Global Vegetation Index Guide. NOAA National Climatic Data Center, Ashville, North Carolina, USA.
- PINZON, J.E., BROWN, M.E. and TUCKER, C.J., 2005, Satellite time series correction of orbital drift artifacts using empirical mode decomposition. In *EMD and its Applications*, N.E. Huang and S.S.P. Shen (Eds) (Singapore: World Scientific Publishers) (in press).
- POVEDA, G. and SALAZAR, L.F., 2005, Annual and interannual (ENSO) variability of spatial scaling properties of a vegetation index (NDVI) in Amazonia. *Remote Sensing of Environment*, **93**, pp. 391–401.
- RAO, C.R.N. and CHEN, J., 1995, Inter-satellite calibration linkages for the visible and near-infrared channels of the Advanced Very High Resolution Radiometer on the NOAA-7, NOAA-9 and NOAA-11 spacecraft. *International Journal of Remote Sensing*, **16**, pp. 1931–1942.
- ROSEN, J., KJOME, N.T., MCKENZIE, R.L. and LILEY, J.B., 1994, Decay of Mount Pinatubo aerosol at midlatitudes in the northern and southern hemispheres. *Journal of Geophysical Research*, **99**, pp. 25733–25739.
- RUSSEL, P.B., LIVINGSTON, J.M., DURRON, E.G., PUESCHEL, R.F., REAGAN, J.A., DEFOOR, T.E., BOX, M.A., ALLEN, D., PILEWSKIE, P., HERMAN, B.M., KINNE, S.A. and HOFMANN, D.J., 1993, Pinatubo and pre-Pinatubo optical-depth spectra: Mauna Loa measurements, comparisons, inferred particle size distributions, radiative effects, and relationships to lidar data. *Journal of Geophysical Research*, **98**, pp. 22969–22985.
- SAINT, G., 1995, Spot-4 vegetation system—association with high-resolution data for multiscale studies. *Advances in Space Research*, **17**, pp. 107–110.
- SALEOUS, N.Z., VERMOTE, E.F., JUSTICE, C.O., TOWNSHEND, J.R.G., TUCKER, C.J. and GOWARD, S.N., 2000, Improvements in the global biospheric record from the advanced very high resolution radiometer. *International Journal of Remote Sensing*, **21**, pp. 1251–1278.
- SATO, M., HANSEN, J., MCCORMICK, M.P. and POLLACK, J.B., 1993, Stratospheric aerosol optical depths, 1850–1990. *Journal of Geophysical Research*, **98**, pp. 22987–22994.
- SCHNEIDER, S.R., MCGINNIS, D.F. and GATLIN, J.A., 1981, Use of NOAA AVHRR Visible and Near-Infrared Data for Land Remote Sensing. NOAA Technical Report NESS 84, NOAA National Earth Satellite Service, Washington, DC.

- TANRE, D., HOLBEN, B.N. and KAUFMAN, Y.J., 1992, Atmospheric correction algorithm for NOAA-AVHRR products: theory and applications. *IEEE Transactions on Geoscience and Remote Sensing*, **30**, pp. 2231–2248.
- TARPLEY, J.P., SCHNEIDER, S.R. and MONEY, R.L., 1984, Global vegetation indices from NOAA-7 meteorological satellite. *Journal of Climate and Applied Meteorology*, **23**, pp. 491–494.
- TOWNSHEND, J.R.G., 1994, Global data sets for land applications from the advanced very high resolution radiometer: an introduction. *International Journal of Remote Sensing*, **15**, pp. 3319–3332.
- TOWNSHEND, J.R.G. and TUCKER, C.J., 1981, Utility of AVHRR NOAA-6 and -7 for vegetation mapping. In *Proceedings of the International Conference on Matching Remote Sensing Technologies and Their Applications* (London/Nottingham: Remote Sensing Society), pp. 97–109.
- TUCKER, C.J., 1979, Red and photographic infrared linear combinations for monitoring vegetation. *Remote Sensing of Environment*, **8**, pp. 127–150.
- TUCKER, C.J., NEWCOMB, W.W. and DREGNE, H.E., 1994, Improved data sets for determination of desert spatial extent. *International Journal of Remote Sensing*, **15**, pp. 3519–3545.
- VERMOTE, E.F. and KAUFMAN, Y.J., 1995, Absolute calibration of AVHRR visible and near-infrared channels using ocean and cloud views. *International Journal of Remote Sensing*, **16**, pp. 2317–2340.
- VERMOTE, E., SALEOUS, N.E., KAUFMAN, Y.J. and DUTTON, E., 1997, Data preprocessing: stratospheric aerosol perturbing effect on the remote sensing of vegetation: correction method for the composite NDVI after the Pinatubo eruption. *Remote Sensing Reviews*, **15**, pp. 7–21.